Coarse-Grained Modeling of the Actin Filament Derived from Atomistic-Scale Simulations

Jhih-Wei Chu and Gregory A. Voth
Center for Biophysical Modeling and Simulation and Department of Chemistry, University of Utah, Salt Lake City, Utah

ABSTRACT A coarse-grained (CG) procedure that incorporates the information obtained from all-atom molecular dynamics (MD) simulations is presented and applied to actin filaments (F-actin). This procedure matches the averaged values and fluctuations of the effective internal coordinates that are used to define a CG model to the values extracted from atomistic MD simulations. The fluctuations of effective internal coordinates in a CG model are computed via normal-mode analysis (NMA), and the computed fluctuations are matched with the atomistic MD results in a self-consistent manner. Each actin monomer (G-actin) is coarse-grained into four sites, and each site corresponds to one of the subdomains of G-actin. The potential energy of a CG G-actin contains three bonds, two angles, and one dihedral angle; effective harmonic bonds are used to describe the intermonomer interactions in a CG F-actin. The persistence length of a CG F-actin was found to be sensitive to the cut-off distance of assigning intermonomer bonds. Effective harmonic bonds for a monomer with its third nearest neighboring monomers are found to be necessary to reproduce the values of persistence length obtained from all-atom MD simulations. Compared to the elastic network model, incorporating the information of internal coordinate fluctuations enhances the accuracy and robustness for a CG model to describe the shapes of low-frequency vibrational modes. Combining the fluctuation-matching CG procedure and NMA, the achievable time- and length scales of modeling actin filaments can be greatly enhanced. In particular, a method is described to compute the force-extension curve using the CG model developed in this work and NMA. It was found that F-actin is easily buckled under compressive deformation, and a writhing mode is developed as a result. In addition to the bending and twisting modes, this novel writhing mode of F-actin could also play important roles in the interactions of F-actin with actin-binding proteins and in the force-generation process via polymerization.

INTRODUCTION

Actin filaments (F-actin) are the most abundant component of the cellular cytoskeleton, and they also play critical roles in numerous processes in eukaryotic cells: cytoskeletal support, cell motility, cell division, endocytosis, and intracellular transportation (1–4). The functions of actin filaments are closely related to its mechanical properties, such as the flexural rigidity. Understanding how the structures and conformation of monomeric building blocks (G-actin) confer the specific properties of F-actin is thus important in the fields of molecular biology and biophysics.

Continuum models based on the linear elastic theory have provided a general framework for characterizing the mechanical properties of the cytoskeleton (1,5–8). However, these models do not consider the atomic details of the composing proteins and ligands, and therefore cannot reveal the structural/property relationship of F-actin. On the other hand, molecular dynamics (MD) simulations with all-atom force fields include microscopic structures and interactions and are suitable for a detailed description of biomolecules (9–11). For example, the DNase I-binding loop (DB-loop) of G-actin adapts a loop conformation in G-ATP (ATP-bound G-actin) (12,13) and folds into an α-helix in G-ADP (ADP-bound G-actin) after ATP hydrolysis and the dissociation of phosphate groups (14). MD simulations (15) on a repeat unit (13 monomers) of F-ATP (F-actin composed of G-ATP) and F-ADP (F-actin composed of G-ADP) have characterized the significant effects of the DB-loop conformation on the structural and mechanical properties of actin filaments. These atomistic simulations also provide valuable insight into the molecular origin of processes that regulate the growth dynamics of F-actin, such as the annealing reaction (16,17). Unfortunately, the accessible time- ($<$100 ns) and length scales ($<$50 nm) of all-atom MD simulations are still limited, which hinders the studies of longer filaments, their growth dynamics, and the interactions of F-actin with motor proteins such as myosin.

One possible solution is to employ coarse-grained (CG) models (11,18–21), in which the details in an all-atom description are reduced, and the accessible scales can be increased. If the essential physics of interested processes are captured, CG simulations can be used to systematically study complicated biological systems. However, it is usually difficult to know a priori the features of a system that need to be included in a CG model. Therefore, it is important to be able to systematically improve a CG model based on the properties and details from a fine-grained (even atomistic-scale) description. In other words, the ability for a CG model to exchange information with the underlying fine-grained description is critical. Such multiscale CG procedures have appeared for soft materials such as the biological membranes

Submitted September 6, 2005, and accepted for publication November 22, 2005.

Address reprint requests to Gregory A. Voth, Dept. of Chemistry, University of Utah, 315 S. 1400 E., Rm. 2020, Salt Lake City, UT 84112-0850. Tel.: 801-581-7272; E-mail: voth@chem.utah.edu.

0006-3495/06/03/1572/11 $2.00

doi: 10.1529/biophysj.105.073924

(22–24), but have not yet been reported for the components of cytoskeleton, such as the actin filament.

F-actin is an assembly of the protein G-actin (375 residues). Until recently (15), the size of F-actin has limited earlier theoretical works at the coarse-grained level (25–27). Due to the stiffness of F-actin (persistence length 12–15 μm for F-ATP and 7–10 μm for F-ADP (28)), the harmonic approximation was usually employed and combined with normal mode analysis (NMA) (29) in the CG studies of F-actin. Common CG representations of F-actin are similar to the elastic network model (ENM) (30–35) that has been widely used for a coarse representation of globular proteins and their complexes. In ENMs, effective harmonic bonds with a universal force constant connect the CG sites of a reference structure that are within a cutoff distance. For modeling protein molecules using ENM, the CG sites are usually chosen to be the α carbons (C_α) and x-ray structures are usually the reference structures. For the modeling of F-actin, a coarser treatment, in which each G-actin monomer represents a CG site, has been employed (27). With the determination of CG sites given a reference structure, two adjustable parameters are involved in the ENM: the cut-off distance of adding effective harmonic bonds and the value of the universal spring constant. Despite its simplicity, the ENM has been shown to be useful in capturing the ''shape'' of low-frequency vibrational modes of a system by using NMA. ENM has also been applied to aid in the refinement of structural models of macromolecules, including F-actin, from low-resolution structural data (25,36–39).

Since the specific properties of actin filaments that endow their biological functions are derived from the protein-protein interactions among actin monomers in an F-actin, a CG model ideally needs to describe these interactions in a physical manner. Protein-protein interactions also confer an F-actin its flexural rigidity, and a CG model should also be able to reproduce its persistence length. It seems apparent that the ENM, with only two adjustable parameters, is not suitable for achieving these goals. First of all, the interactions among difference sites depend on the nature of the local environments and may not be represented by a universal spring constant. An ENM with distance-dependent force constants could be of use, but the functional form of the distance dependence needs to be determined. The cut-off distance within which an effective harmonic bond is applied in an ENM affects both the flexural rigidity and the effective protein-protein interactions, and also needs to be determined. The elastic-network-based approaches therefore require systematic ways of refinement for the CG model to be of use in biophysical simulations of actin filaments. Moreover, the C_α-based ENM may still be too fine-grained for an efficient CG modeling of a long actin filament, whereas the one-monomer/one-site model could be too coarse to describe certain properties of F-actin, such as the polarity at the + and the – ends and its interactions with actin binding proteins. Therefore, an intermediate resolution CG model of F-actin should prove to be quite valuable.

In this work, a new intermediate-resolution CG model of an actin filament is developed (Fig. 1). Each monomer is composed of four CG ''particles''; each corresponding to one of the subdomains of G-actin. The basic topology of the actin monomer is thus preserved at this scale of resolution, and the important emerging behaviors from ATP hydrolysis or interactions with motor proteins can also be represented effectively. The subdomain description of G-actin has also been widely used in the structural analysis of F-actin (12–14, 40–43). The effective interactions of a CG actin monomer in this work include three harmonic bonds that connect D2 and D1 (see the captions of Fig. 1 for the definitions of

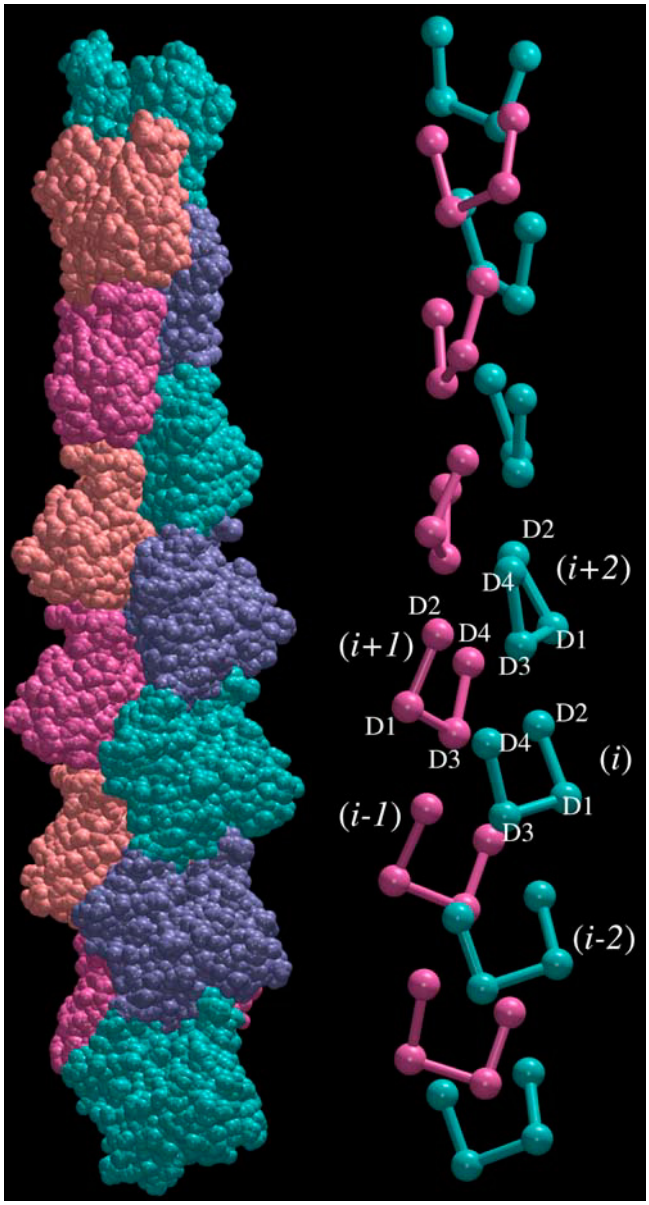

FIGURE 1 Atomic model of F-actin (*left*) of Holmes et al. (40) and the CG representation (*right*). Each actin monomer has four sites denoted as Dn, where n = 1–4. Actin monomers are denoted by italic numbers.

abbreviations), D1 and D3, and D3 and D4, two harmonic angles of D2-D1-D3 and D1-D3-D4 that represent the open/closed conformations of the ATP cleft of G-actin, and a dihedral angle of D2-D1-D3-D4 that corresponds to the mode of propeller rotation of G-actin. The use of six effective internal coordinates in the CG model of G-actin is also consistent with the number of independent vibrational modes of a four-particle molecule. Interactions between actin monomers in a filament are described by effective harmonic bonds similar to that of the ENM but without assuming a universal force constant or a particular form of distance dependence.

After defining the CG sites and the forms of interaction potentials, the process of obtaining these force fields then determines a CG model. In this work, a new procedure is devised to obtain the effective CG force fields from all-atom simulations. The procedure is based on matching the fluctuations of the effective internal coordinates (EIC) that are chosen to describe a CG model to the fluctuations extracted from the all-atom MD trajectories. The fluctuations of EICs in a CG model can be calculated via NMA, and the effective force constants in a CG model are then adjusted in a self-consistent manner to reproduce the target fluctuations. This procedure is also a way to match the vibrational modes of a CG model to the quasiharmonic modes (29) from atomistic MD simulations by using the EICs as basis functions. This procedure endows a CG model with a ''multiscale'' nature such that the information at the atomic level is systematically propagated to the mesoscopic-scale (CG) representation, and will be referred to as the fluctuation-matching method in the following sections of this article. The results of such multiscale coarse-graining of actin filaments may also provide valuable insight in the coarse-graining of larger components of the cytoskeleton such as microtubules for which all-atom MD simulations may not be feasible.

In the next section, details of the fluctuation-matching procedure and the computation of persistence length of an actin filament are described. Examination of various aspects of the CG model will then be presented in the Results section as will an example of using the CG model to study the behavior of F-actin at longer and larger scales, namely the force-extension curves of F-actin. Finally, conclusions will be given.

METHODS

In this section, the procedures of developing CG models of F-actin are described in detail. The methods for computing the persistence lengths of CG F-actin are also reported.

The CG model

The CG model shown in Fig. 1 contains four sites per actin monomer, and each site corresponds to one of the four subdomains of G-actin. The adenosine group of ATP or ADP is incorporated into D3 and the phosphate groups are incorporated into D4. Three bonds, two angles, and one dihedral angle compose the intramonomer potential, so that important slow modes of motion of G-actin, such as the propeller rotation and the opening/closing of the ATP cleft, are incorporated in a straightforward manner. Effective harmonic bonds are used to connect the monomers in an F-actin. Between each pair of CG monomers, there can be 16 (4×4) types of effective harmonic bonds, all of which are considered explicitly. This generalization allows one to evaluate the limitations of using a universal force constant in the ENM.

The structure of F-actin is shown in Fig. 1. The Holmes model developed by x-ray fiber diffraction indicates that F-actin is a left-handed helix with a rotation of 166° and a rise of 27.5 Å (40). F-actin can also be viewed as two right-handed helices wound together. Each monomer is in direct contact with four neighbors in the filament as shown in Fig. 1, two from the same right-handed helix that a monomer locates and two from the opposite helix. Therefore, effective harmonic bonds should be placed between monomers i and $i \pm 1$ in the opposite helix and i and $i \pm 2$ along the same helix. With reduced degrees of freedom and the simplified forms of interactions, it is possible that additional interactions are required in the CG model to reproduce certain properties of F-actin. Since the force constants of EICs are going to be determined by the fluctuation-matching procedure, the cutoff distance, R_k, within which an effective harmonic is placed is thus the adjustable parameter of the model. To examine the influence of R_k on the properties of the CG F-actin, models with different values of R_k have been built and analyzed. Different R_ks in the CG models of F-actin are represented by the largest interval between two monomers that exhibit effective harmonic bonds, and all 16 effective bonds between any two pairs of monomers are explicitly considered. In this work, the largest interval that has been studied is 6; that is, monomer i in the filament can have effective bonds with monomers $i \pm m$, where $m = 1$–6.

Parametrization of the effective force fields via the fluctuation-matching method

The details of the all-atom MD simulations of a 13-monomer repeat of both F-ATP and F-ADP under periodic boundary conditions have been reported elsewhere (15). The MD simulations of F-actin contain 575,000 atoms, including explicit solvent molecules, and trajectories of 40 ns have been generated (15). The center of mass of the subdomains of F-ATP and F-ADP were extracted from the last 10 ns of the all-atom trajectories. The CG versions of the all-atom (CG-AA) trajectories then provide the target data for developing the coarse-grained models of an actin filament.

The equilibrium values of EICs, are obtained from the corresponding averages obtained from CG-AA trajectories. For each EIC, the fluctuations can also be calculated, $\langle \delta EIC_i^2 \rangle = \langle (EIC_i - \langle EIC_i \rangle)^2 \rangle$, from CG-AA trajectories, and are the target data to determine the effective force constants of a CG model. Since the fluctuations of EICs in a CG model can also be computed via NMA (29), the effective force constants in a CG model are determined by matching the fluctuations computed from NMA to that obtained from CG-AA trajectories. The number of unknowns thus equals the number of EICs in a CG model.

It is important to note that the fluctuation of an EIC depends not only on its own force constant, but also on the force constants of other EICs. This is because the CG models that are employed in this work contain a network of interconnected harmonic bonds. Therefore, the following iterative relationship was utilized to obtain a self-consistent solution for the force constants in a CG model:

$$k_j^{n+1} = k_j^n + \alpha \times (\delta EIC_j^n - \delta EIC_j^{CG-AA}), \qquad (1)$$

where k_j is the force constant of the j^{th} EIC in a CG model, δEIC_j is the fluctuation of the j^{th} EIC computed from NMA, and δEIC_j^{CG-AA} is the fluctuation of the j^{th} EIC extracted from CG-AA trajectories. The superscript n denotes the number of an iteration step, and α is a positive numerical factor. The philosophy is that even if k_j affects the fluctuations of all other EICs, its effects on the j^{th} EIC should be most significant; the interdependence of EICs are incorporated by using Eq. 1. Furthermore, the allowed values of force constants are limited to positive numbers or zero; therefore,

the force constant of an EIC becomes stationary only if the computed fluctuation matches with the all-atom result or if it is decreased to zero. A force constant of zero indicates that the fluctuation of an EIC is still smaller than that in CG-AA trajectories, even if its force constant is reduced to zero, and such an EIC is considered redundant in a CG model and is automatically picked up during the self-consistent iterations. The fluctuation-matching procedure is thus a systematic way to mimic the pattern of internal coordinate fluctuations in all-atom simulations, and the number of EICs whose fluctuations match with those in all-atom simulations is maximized in a CG model. The fluctuations of the EICs with a force constant of zero are underestimated, and these EICs are considered redundant. A mismatching of the fluctuations of certain EICs is inevitable with the reduction of degrees of freedom and the simplification of using effective harmonic interactions.

Since periodic boundary conditions were applied in the all-atom simulations for a repeat of F-actin with 13 monomers, each type of internal coordinate, an iD2-(i + 2)D1 bond (see Fig. 1), for example, has 13 distinct copies in these atomistic simulations. Due to the limited timescale of sampling and/or the fact that an enforced periodic crossover every 13 monomers is a source of frustration for F-actin (the twist of F-actin appears to be random with magnitude of fluctuation around 5° (44)), not all 13 copies of a specific type of EIC have the same averages and fluctuations in the CG-AA trajectories. To examine the CG procedure regardless of this issue, two sets of CG models have been built and analyzed. In the first set, each of the 13 copies of a particular EIC in the atomistic MD simulations is treated independently, i.e., for a CG model containing effective harmonic bonds between monomer i and $i \pm m$, where $m = 1$–6, there can be a total of 1248 ($16 \times 6 \times 13$) types of intermonomer bonds. In the second set, all 13 copies of a type of EIC have the same value of force constant and equilibrium length, and the target data of fluctuations are root mean-square averaged over the 13 copies in CG-AA trajectories.

The basic unit of the CG model is thus a 13-monomer fragment of F-actin. The boundary effects of the 13-monomer fragment disappear with a minimal number of repeats of three, since each repeat only interacts with the neighboring ones. The fluctuations of EICs from NMA of the middle fragment in a three-repeat filament were also found to be identical to those of a five-repeat or a seven-repeat filament. The three-repeat filament was thus used to develop the CG parameters from the all-atom simulations.

Computation of persistence lengths

The persistence length (L_p) is an important material property of the actin filament and is closely related to its biological functions. NMA provides the solutions of equations of motion under the harmonic approximation, and thus the configurations of a CG model corresponding to arbitrary timescales at 310 K can be generated from the eigenvalues and the eigenvectors obtained from NMA (29). Specifically, trajectories corresponding to 10 times the period of the slowest modes are generated using a time step of one-tenth of the period of the slowest mode. Different trajectories are obtained by assigning randomly the initial phases of the vibrational modes. For a CG model of three repeats of F-actin, this set of configurations corresponds to a trajectory of 500 ns; for a CG F-actin of a length of 1 μm, these configurations correspond to a trajectory of 50 μs. Increasing the length of each trajectory or the number of independent trajectories did not change the results of the computed persistence length.

To compute L_p, the four-site-per-monomer model is mapped into a linear polymer based on the following procedure. The center of mass of monomer i at one of the two right-handed helices is first calculated, and the centers of mass of monomers i-1 and i + 1 at the opposite strand are then calculated, averaged, and denoted as i'. The center between i and i', whose position is denoted as r_i, is used to define the corresponding position of monomer i along the linear polymer. The contour length of the polymer is defined as the sum of the distances of each segment (r_i, r_{i+1}). The tangent vectors along a polymer are computed from these r_is, and the bending angles along a filament are determined. The effects of spontaneous curvatures due to the mapping procedures are taken into account as described in Chu and Voth (15). The persistence length of an F-actin is computed directly from the slope of exponential decay of the ensemble-averaged cosine of bending angle fluctuations as a function of the contour length, i.e.,

$$\langle \cos(\theta(s) - \theta_0(s)) \rangle = \exp\left(-\frac{s}{L_p}\right). \quad (2)$$

Such exponential decay for a four-site-per-monomer CG model as described in Fig. 1 is shown in Fig. 2; it is apparent that Eq. 2 is suitable to describe the flexural rigidity of the CG F-actin developed in this work.

The NMA and other analyses of the CG models were performed using CHARMM software (10) and the visual molecular dynamics program (45) was used for the visualization and graphics of F-actin.

RESULTS

Using the fluctuation-matching procedure, CG models of F-ATP (ATP bound F-actin) and F-ADP (ADP bound F-actin) can be built with the parameters determined directly from atomistic MD simulations. Models in which the 13 copies of a particular type of EIC (an iD2-(i + 1)D1 bond, for example; see Fig. 1) are treated independently are denoted as A_i; models in which the 13 copies of an EIC type have the same parameters are denoted as B_i. The subscript denotes the largest interval between two monomers to have effective bonds in a CG model. For example, a monomer i in the A_6 model has intermonomer bonds with monomers $i \pm m$, where $m = 1$–6. The total number of bond types for the intermonomer interactions in A_6 is thus 1248.

The results presented below are for isolated CG F-actin (without using periodic boundary conditions) composed of three repeat units with a total of 39 monomers and a length of 106 nm. CG models as long as 1 μm (30 repeat units) have also been built using the parameters obtained from the aforementioned procedure. The results indicate that material properties of the four-sites-per-monomer CG model are indeed independent of the length of an F-actin.

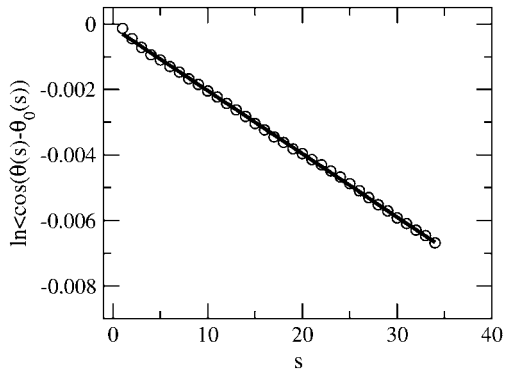

FIGURE 2 Log of the cosine function of binding angles of an F-actin as a function of its contour length. $\theta(s)$ is the bending angle at contour length s, and $\theta_0(s)$ is the equilibrium angle at s. In the x axis, the contour length, s, is normalized by the average length corresponding to each monomer, δs_0; that is, the contour length is represented as the number of G-actin monomers along an actin filament.

The self-consistent iterations for solving force constants using Eq. 1 usually converge within 1000 steps, with the maximum relative error with respect to the target data being $<0.5\%$. The intramonomer parameters converge much more quickly (<50 steps) and match the all-atom MD data essentially exactly. The above phenomena were found to be independent of the number of intermonomer degrees of freedom. As mentioned previously, for the intermonomer bonds with a force constant of zero, the fluctuations are underestimated compared to the target data. The percentages of underestimation of these degrees of freedom relative to the target data are averaged and reported in Table 1. As shown in Table 1, the more effective the bonds that are included, the higher the averaged percentage of underestimation, but the incremental increase decays as the added effective bonds become longer. The A_6 model results in an averaged underestimation of 10.6% for F-ATP and 14.1% for F-ADP. When the parameter of an EIC is obtained by averaging over the 13 copies in a repeat, the underestimation of fluctuations becomes lower. For F-ATP, the B_6 model gives an average underestimation of 4% for F-ATP and 5% for F-ADP.

Persistence lengths of coarse-grained actin filaments

The computed persistence lengths of different CG models of F-actin are shown in Fig. 3. For the *A* and *B* models of both F-ATP and F-ADP, the flexural rigidity of a CG F-actin increases monotonically with the number of intermonomer bonds. Including effective bonds only with the nearest neighbor across the strand for a monomer (the i-($i \pm 1$) interactions) in, i.e., the A_1 and B_1 models, the resulting persistence lengths are 7–8 times smaller than the results of atomistic MD simulations. The ATP-hydrolysis-induced conformational change of the DB loop weakens the cross-strand interactions as delineated by the all-atom MD simulations (15), and these changes of interactions translate into smaller values of force constants in a CG model. Compared to atomistic MD simulations, force constants of the A_1 models of F-ATP and F-ADP lead to a similar relative strength of flexural rigidities, even though the absolute value of each is smaller than the all-atom result.

TABLE 1 Averaged relative underestimation of fluctuations (%) for the internal coordinates that have a force constant of zero compared to the CG-AA results

Model	F-ATP	F-ADP	Model	F-ATP	F-ADP
A_1	2.1	2.0	B_1	1.2	0.4
A_2	3.7	4.5	B_2	1.1	1.7
A_3	6.3	7.5	B_3	2.4	2.5
A_4	8.3	9.9	B_4	2.9	3.6
A_5	9.7	11.6	B_5	3.7	4.3
A_6	10.6	14.1	B_6	4.0	5.0

Both the *A* and *B* CG models for F-ATP and F-ADP are shown.

Adding effective bonds for a monomer with its nearest neighbor monomer along the same protofilament (the i-($i \pm 2$) interactions in Fig. 1), the A_2 and B_2 models, increases the persistence lengths by three to four times, indicating that the interactions along each protofilament are important in conferring the elasticity of an actin filament. However, the resulting flexural rigidity of A_2 and B_2 is still 1–2 times smaller than the atomistic results, even when all possible effective bonds among actin monomers that are in direct contact have been included. Therefore, with a reduced number of degrees of freedom and the simplification of interactions in CG modeling, criteria simply based on physical inspection may not be enough to capture certain important properties of F-actin. Although the force constants of A_2 and B_2 models could be scaled to reproduce the desired values of persistence length, it is one of the goals of this study to explore the possibility of reproducing both the fluctuations of EICs and the flexural rigidity of F-actin.

Going beyond the nearest neighbor connections does increase the flexural rigidity of CG filaments as shown in Fig. 3. With effective bonds connecting a monomer with its first to third nearest monomers, the computed persistence length of the A_6 model of F-ATP is 16.2 μm, in good agreement with the atomistic MD result (15.8–16.5 μm (15)). It can also be seen from Fig. 3 that the incremental increase of L_P of CG F-ATP decays with the inclusion of longer effective bonds. This result is due to the fact that the force constants of the effective bonds decrease with its equilibrium length; more details of the distance dependence of the force constants will be discussed later. For F-ADP, on the other hand, the A_4 ($L_p = 9.68$ μm), A_5 ($L_p = 10.7$ μm), and A_6 ($L_p = 13.8$ μm) models overestimate the persistence length compared to the MD result (8.73 μm), but the A_3 ($L_p = 6.83$ μm) model underestimates it. Since the CG procedure generally underestimates the fluctuations of certain internal coordinates (those with a force constant of zero), it is thus possible that it overestimates the flexural rigidity. For F-ATP such an overestimation did not occur in both *A* and *B* models, possibly because the over restraint of certain degrees of freedom is compensated by the loss of integrity due to the reduced degrees of freedom. For F-ADP, on the other hand, the presence of structural distortion and defects caused by the change of the DB-loop conformation (15) increases the heterogeneity of the filament. As a result, matching the fluctuations of some internal coordinates may lead to more significant underestimation of the fluctuations of others and lead to an overestimation of L_p. Indeed, the percentages of underestimated fluctuations of the zero-force-constant EIC are higher for F-ADP than for F-ATP as shown in Table 1. After the heterogeneity is removed in the corresponding B models of F-ADP by averaging the parameters of an EIC over the 13 copies in a repeat, the resulting persistence lengths of the B_6 models agrees well with the atomistic MD results, as shown in Fig. 3.

The computed persistence lengths of CG F-actin (in B_6 models, for F-ATP, 14.4 μm, for F-ADP, 8.7 μm) are in

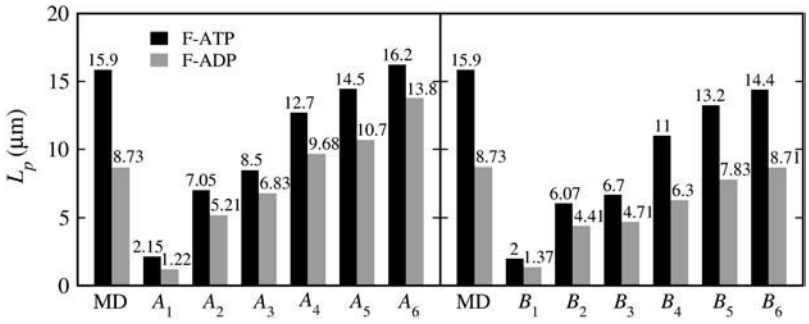

FIGURE 3 Persistence lengths of the *A* models *(left)* and the *B* models (*right*; see text for definitions of the models) of the CG F-ATP (*solid*) and F-ADP (*shaded*). The values computed from all-atom simulations are also labeled.

good agreement with the experimental measurements (for F-ATP, 13.5 μm, for F-ADP, 9 μm (28)). In addition to flexural rigidity, the torsional rigidity, κ_T (F-ATP: $\kappa_T = 2.2 \times 10^{-26}$ N•m^2; F-ADP: $\kappa_T = 1.8 \times 10^{-26}$ N•m^2), which was not used as a target property during the parametrization of CG F-actin, is also in good agreement with experimental measurements ($\kappa_T = 2.8 \times 10^{-26}$ N•m^2 for Mg^{2+} bound F-actin and 8.5×10^{-26} N•m^2 for Ca^{2+} bound F-actin with the presence of phalloidin-tetramethylrhodamine (46)) and earlier theoretical models ($\kappa_T = 2.6 \times 10^{-26}$ N•m^2 (47)).

The above results indicate that other than modifying the force constants of the effective bonds, the cutoff radius, R_k, of assigning these bonds can also be used to adjust the flexural rigidity of a CG F-actin. The force constants of the CG F-actin are obtained by matching the fluctuations of EICs in all-atom simulations, and more extensive CG bonds than those suggested by physical inspection are needed to reproduce the flexural rigidity. It was found that CG models with effective bonds between a monomer and its first to third nearest monomers provide quantitative agreement in persistence length with the all-atom simulations and experimental measurements. It is thus possible for a CG F-actin to reproduce both the pattern of EIC fluctuations and the elastic properties from the fine-grained MD description by using the fluctuation-matching method.

The current models use harmonic bonds to describe the interactions among the actin monomers in an F-actin, and the self-consistent iterative procedure of Eq. 1 generates a pattern of EIC fluctuations that best matches the target data. It was also found that the force constants that result from the CG procedure decrease with their equilibrium lengths. As a result, the properties of the CG model should reach convergence when more effective bonds are included, and thus enable systematic refinement of a CG model. The details of the relationship between the force constants of the effective CG bonds and their equilibrium lengths are presented in the following section.

Dependence of the force constants on the equilibrium lengths of the effective bonds

The force constants, k, of the intermonomer harmonic bonds in the B_6 models of F-ATP and F-ADP are plotted as a function of their equilibrium length, b_0, in Fig. 4. Similar behavior has been found in other models. The intermonomer effective bonds are divided into two groups in Fig. 4. The first group (G1) contains the bonds between monomers that are in direct contact (the i-($i \pm 1$) and i-($i \pm 2$) interactions), and the second group (G2) contains the rest of the bonds. The G1 bonds are plotted as solid circles in Fig. 4, and the G2 bonds are plotted as open circles. For the effective bonds in the G1 group, the force constants decay with their equilibrium length, and a power law expression was found to describe the data better than an exponentially decaying function. The orders of decay for the force constants of G1 bonds with b_0 were found to be 3.22 for F-ATP and 1.8 for F-ADP (Fig. 4, *solid lines*). For G2 bonds, the force

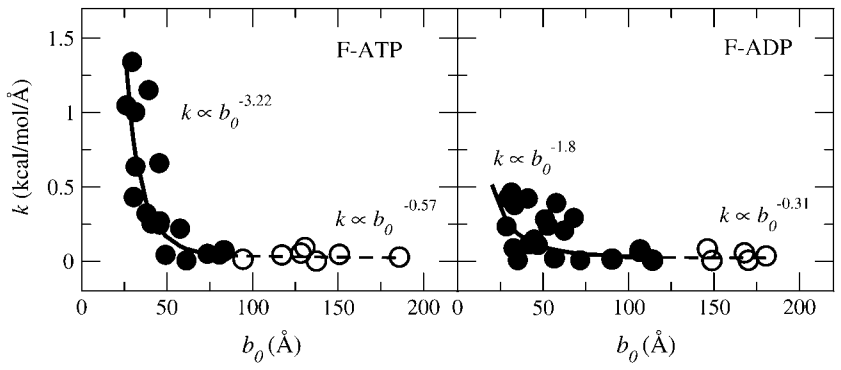

FIGURE 4 Force constant, k, of the effective bonds in the B_6 model of F-ATP (*left*) and F-ADP (*right*) as a function of their equilibrium length, b_0. The effective bond between a monomer and its nearest neighbor monomers is shown as solid circles. The longer-range effective bonds, including the interactions with the second and third nearest monomers are shown in open circles. The fitted scaling orders of k and a function of b_0 for the solid circles and the open circles are also shown.

constants also decay with their equilibrium lengths but with smaller orders, 0.57 for F-ATP and 0.31 for F-ADP (Fig. 4, *dashed lines*).

The decay of force constants with the lengths of effective bonds indicates that the proposed CG procedure would result in convergent properties. However, the rates of decay become slow when they go beyond the nearest-monomer effective bonds (75–~80 Å), and this tendency makes the convergence difficult. A decay order <1 also indicates that although the long-range effective bonds have smaller force constants, their effective elasticity is higher. This is also the reason that adding longer effective bonds could increase the persistence lengths by 1–2 times going from A_2 and B_2 models to A_6 and B_6 models.

From the above analysis, the following strategy can be suggested for developing CG models of large bioassemblies using an elastic-network type of interactions, such as microtubules, for which all-atom MD simulations may not be feasible. The specific pattern of the protein-protein interactions, such as the order of power-law decay of the force constants as a function of their equilibrium lengths, can be obtained by performing MD simulations on small clusters of the composing protein monomers (for example, a cluster of a tubulin with its nearest neighboring monomers). A material property such as the flexural rigidity is more sensitive to the effective interactions of a longer range, and these interactions could be adjusted so that a CG model has the desired flexural rigidity.

Although long-range harmonic interactions are required to describe the flexural rigidity of a CG F-actin, it is not the case for describing the structural properties of a filament. For example, even for the A_1 model of F-ATP that has the fewest number of effective bonds, the equilibrium structure only has a root mean-square deviation of 0.065 Å compared to the averaged structure from all-atom MD simulations, and 0.056 Å compared to the structure of the A_6 model. Therefore, it can be inferred from the above result that for the purpose of using CG models to refine the model development from low-resolution structural data, it is sufficient to incorporate only the nearest monomer interactions in the case of actin filaments. It is also suggested that a power-law expression of the force constant as a function of their equilibrium lengths, with the power-law order as an adjustable parameter, can be useful to enhance the quality of model refinement.

Comparison with the quasiharmonic modes from all-atom MD simulations

One of the purposes of CG modeling of macromolecules is to describe the motions or fluctuations that are related to their biological functions. In the framework of the harmonic approximation, a few slow modes contribute a significant portion of the total fluctuations (29,48,49). The success of using simple models, such as the elastic-network model (ENM), in characterizing the function-related motions of certain globular proteins has encouraged the use of coarse-grained descriptions in modeling large biological systems (30–35). However, due to the lack of all-atom MD simulations for such systems, it is difficult to evaluate the accuracy of a simplified model such as the ENM in describing large biological systems such as actin filaments. Compared to the ENM, the fluctuation-matching method proposed in this study systematically incorporates the information of internal coordinate fluctuations obtained from all-atom simulations in addition to the structural information. It is thus interesting and valuable to compare how the proposed fluctuation-matching approach could improve the performance of the ENM in terms of characterizing the shapes of low-frequency vibrational modes of F-actin.

From the all-atom MD simulations of a repeat (13 monomers) of F-ATP and F-ADP, the quasiharmonic modes of motion (QHM) can be obtained (29). These QHMs are represented as orthogonal unit vectors with a dimension of 156 ($13 \times 4 \times 3$), and are ranked according to their frequencies (eigenvalues) starting from the slowest mode. The harmonic modes (HM) of motion of the CG models are obtained by NMA, and the comparison of HMs and QHMs provides a measure of the ability of a CG model to capture the shapes of low-frequency vibrational fluctuations. The magnitude of the dot product between a particular QHM and an HM ($|\text{QHM} \cdot \text{HM}|$) can be used to quantify the comparison. Since low-frequency vibrational modes are of major concern, Fig. 5 shows the $|\text{QHM} \cdot \text{HM}|$ of mode 1 (the slowest vibrational mode) and the averaged $|\text{QHM} \cdot \text{HM}|$ of modes 1–5 for both F-ATP and F-ADP. The A models are used to obtain the HM of a repeat of F-ATP and F-ADP under periodic boundary conditions, since the equilibrium structure of the A models has very small root mean-square deviations (<0.1 Å) with the averaged structure from the MD results. The results of $|\text{QHM} \cdot \text{HM}|$ of the ENM are also obtained by replacing the force constants of effective bonds in the A models with a universal constant, and are also shown in Fig. 5 (*right-hand panels*). Note that the shapes of the eigenvectors do not depend on the magnitude of the force constant.

For mode 1 of F-ATP, the CG HM gives a $|\text{QHM} \cdot \text{HM}|$ value of 0.8–0.85 (80–85% similarity) if going beyond the nearest-monomer interactions, i.e., the A_3 model and higher (see Fig. 5, *left-hand panels*). The averaged $|\text{QHM} \cdot \text{HM}|$ values of modes 1–5 also reach a value of ~0.5 for the A_3 model and beyond. Adding more effective bonds only gives a slight increase in $|\text{QHM} \cdot \text{HM}|$, indicating the limitation of using the harmonic form of interactions. However, with the information of internal-coordinate fluctuations from all-atom simulations, the HMs of the A models do have increasingly better performance as the cut-off of effective bonds increases. For the ENM, on the other hand, the values of $|\text{QHM} \cdot \text{HM}|$ are not a regular function of R_k. The best values of $|\text{QHM} \cdot \text{HM}|$ for F-ATP occur in the A_2 model (mode 1, $|\text{QHM} \cdot \text{HM}| = 0.71$, modes 1–5, $|\text{QHM} \cdot \text{HM}| = 0.47$), in which only the nearest-monomer harmonic interactions are included. Even though by using ENM one could

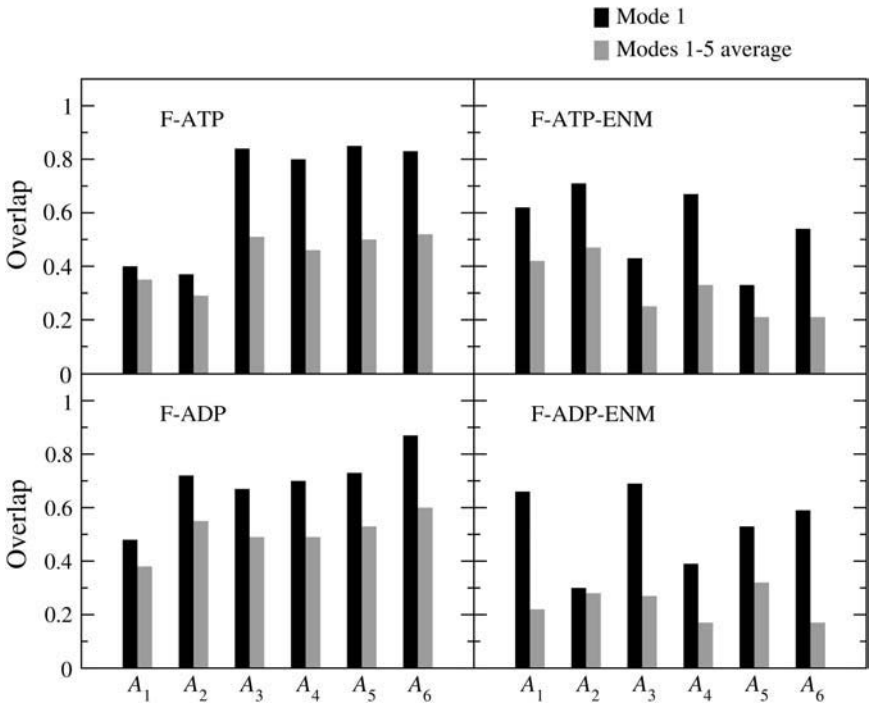

FIGURE 5 Dot products of the vibrational eigenvectors computed from the NMA of the A_6 CG model to that from the quasiharmonic analysis of the all-atom MD trajectories. The values of Mode 1 (the mode with the smallest vibrational frequency; *solid*) and the averaged values of modes 1–5 (*shaded*) are shown for both F-ATP (*left*) and F-ADP (*right*).

get a reasonably good description of the low-frequency vibrational modes, it is not known a priori what would be the optimal R_k to use for a particular system; the values of |QHM • HM| by using the ENM for F-actin can differ by 50% by changing R_k. There also does not exist a clear pattern of the |QHM • HM| values of ENM as a function of R_k in Fig. 5. Employing the fluctuation-matching CG procedure not only improves the robustness of predicting the shape of low-frequency vibrational modes, it also improves the similarity of mode 1 to that of the QHM by 12% and the average of modes 1–5 by 4% compared with the best result of using ENM.

For the case of F-ADP, the CG models from the fluctuation-matching procedure show trends similar to those for F-ATP. The |QHM • HM| value has reached 0.87 for mode 1 and 0.6 for modes 1–5 in the A_6 model. For the ENM, on the other hand, the best value of |QHM • HM|, 0.69 for mode 1 (18% less than the result of using the fluctuation-matching procedure) occurs in A_3, but the optimal choice for the average of modes 1–5 occurs at A_5 (0.32, 28% less than the result of using the fluctuation-matching procedure), and these optimal cut-offs are also different from that of F-ATP.

The above results indicate that the performance of ENM is sensitive to the choice of R_k; choices other than the optimal one can lead to results that are worse by as much as 50%. The optimal choice of R_k is also different for F-ATP and F-ADP, and no obvious rule can be inferred from the results shown in Fig. 5. By incorporating the internal-coordinate fluctuations from all-atom simulations in a self-consistent manner, the robustness of the CG model can be significantly enhanced, and the results are also quantitatively better by 10–30% as measured by the values of |QHM • HM|.

Bridging time- and length scales using CG simulations

The fluctuation-matching procedure proposed in this work couples the results of all-atom simulations to CG models via self-consistent iterations, thus bridging the microscopic and the mesoscopic scales. The NMA provides the exact solutions of equations of motion under the harmonic approximation, which is the basis of the linear elastic theory that has been widely used to describe the mechanical properties of bioassemblies. The NMA thus prevents the need to perform MD or Monte Carlo simulations to obtain configurations for computing properties of a system. Therefore, the CG model also bridges the time-scales by extending the short-time information from the all-atom simulations to the long-time behavior of F-actin using NMA. In this section, a method for computing the force-extension curves of F-actin using the CG model is presented as an example of using CG modeling to characterize biological systems at significantly longer and larger scales.

The force-extension relationship of linear polymers has been of great interest for the last two decades in exploring the properties of biological polymers such as DNA and the cytoskeleton (50–52). Optical tweezers and atomic-force microscopy (AFM) can be used to constrain the two ends of a linear polymer under a constant length or constant force condition, and the resulting forces or lengths at different states of the polymer are measured. The method described below can be used to obtain the force-extension curve of F-actin under the constant-length conditions using the CG model.

Harmonic bonds between the monomers at the two ends of an F-actin can be used to represent the constraining effects in

optical tweezers or AFM experiments. By using a large value of force constant, the end-to-end distance of F-actin can be constrained to the desired value. The geometries of the modified CG potential are minimized to locate the equilibrium configuration, and NMA is then performed with the modified potential so that the vibrational free energy at an end-to-end distance can be calculated at a given temperature. A force-extension curve can then be obtained from the derivatives of the vibrational free energies of F-actin at different end-to-end distances.

For a CG F-actin of three repeats (39 monomers, 106 nm), the force-extension curves of F-ATP and F-ADP are shown in Fig. 6. The B_6 models are used for the calculations of both F-ATP and F-ADP because they best reproduce the persistence length of F-ATP and F-ADP together. The maximum displacements of the end-to-end distances were chosen to be 4% of the values at equilibrium (106 nm). In the stretching regime (positive extension), and in a small portion of the compression regime (extension $= -0.4$ to -0.6 nm), the F-ATP has a stiffness of 37 pN/nm (per μm), and the corresponding value for F-ADP is 31 pN/nm (per μm). These values are in reasonably good agreement with the experimentally measured value of the stretching stiffness of an actin filament (45 pN/nm/μm) labeled with PHDTMR (phalloidin-tetramethyl rhodamine) (53); phalloidin is known to be a structural stabilizer for the actin-filament and may increase its stiffness. Due to its large persistence length (elastic modulus), the enthalpy dominates the contribution to the stiffness, and the entropic stiffening effects are insignificant. In the compression regime beyond a displacement of 0.4–0.6 nm, the filament starts to buckle (1), and little additional force is required to increase the bend, as shown in Fig. 6. In the presence of the constraining potential, the slowest vibrational mode becomes a writhing mode, whose eigenvalue is negative if the NMA is conducted using the compressed structure but without the constraining potential. Similar results have also been observed for an F-actin as long as 1 μm.

Since it is easy to buckle the actin filament (from Fig. 6, the Euler force (1) is estimated to be 1.68 pN for a filament of a length of 1 μm, and the Euler force of F-ADP is 65% that of F-ATP), it follows that the newly found writhing mode could also be relevant for F-actin under a confined cellular environment in addition to the bending and twisting modes. Furthermore, for the force generation of polymerizing actin filaments, these filaments are under compression, and the writhing mode may also play important roles in the interactions with the actin-binding proteins for the regulation of this process.

DISCUSSION

In this work, a coarse-grained procedure that systematically incorporates the information of atomistic MD simulations is presented and applied to actin filaments. This procedure matches the equilibrium values and fluctuations of the internal coordinates chosen to define a CG model to the values extracted from all-atom MD simulations. The fluctuations of effective internal coordinates in a CG model are obtained via normal-mode analysis. Therefore, this procedure is particularly useful for CG models that employ a harmonic form of potential for its internal coordinates, such as the worm-like chain model for linear polymers and the elastic network model for proteins, although it can also be applied to other forms of potentials in a more approximate fashion.

In applying our CG procedure to the actin filament, the CG sites are chosen to be the subdomains of the actin monomer, and effective harmonic bonds are assigned between the monomers in an F-actin. The force constants are determined by the fluctuation-matching procedure, and thus the cut-off distance of assigning the intermonomer bonds is left as an adjustable parameter. It is demonstrated in this work that certain properties of a system, such as the persistence length, are sensitive to the cut-off distances. For F-actin, it was found that a large cut-off of $\sim$200 Å is needed to reproduce the values of persistence length computed from MD simulations. Such a cut-off corresponds to having effective bonds for a monomer with its third-nearest neighbors. It was also found that the force constants of the effective bonds for a monomer with its nearest monomers decay quickly as a function of their equilibrium lengths with a power law order of 2–3. For the effective bonds for a monomer with its second- and third-nearest monomers, the power law decay of

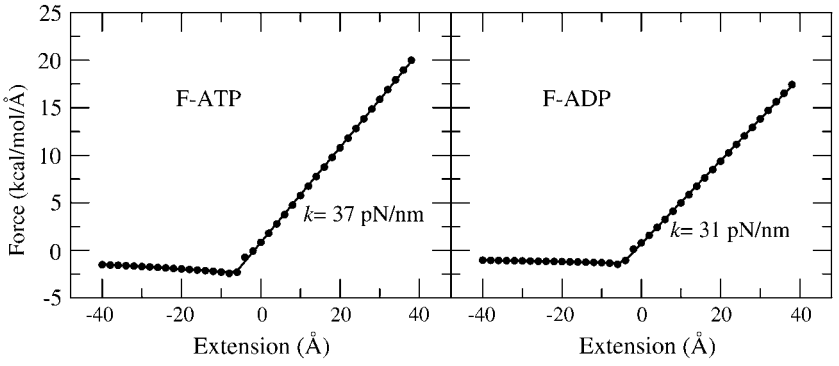

FIGURE 6 Force-extension curves of F-actin with three repeat units ($3 \times 13 = 39$ monomers) of F-ATP (*left*) and F-ADP (*right*). The corresponding stretching stiffness per μm of the filament are also labeled. Under compression, the filament buckles and a writhing mode is developed.

the force constants is slow, with an order <1. However, if the desired objective is only to reproduce the structural properties, using small cut-offs is enough. These observations suggest a general strategy for coarse-graining stiff polymers where the short-range effective interactions can be parameterized from the structural data or from simulations of clusters, and the long-range ones can be used to confer the CG model with the desired elastic properties. For F-actin, a good choice for defining the short-range and the long-range interactions is via physical inspection that the nearest-monomer bonds can be considered as short-range whereas the second- and third-nearest neighbor interactions can be considered as long-range.

Using the fluctuation-matching procedure to incorporate atomic information also enhances the robustness and accuracy of a CG model, in comparison to the ENM approach, to describe the shapes of the fluctuations that are more likely to relate to the functions of a biomolecular system (the low-frequency vibrational modes). The proposed fluctuation-matching method also allows for a more systematic refinement of a CG model. Applying this method to more generalized forms of potentials for coarse-graining the actin filament will be reported in a future work.

By using NMA, the exact solutions of the equations of motion for a system under the harmonic approximation can be obtained, and NMA thus provides a manner to study a system at long timescales (the applicability of the NMA to biological systems has been reviewed elsewhere (36)). Using the fluctuation-matching CG procedure with NMA thus bridges the information obtained at the atomistic microscopic scale to that obtained at the mesoscopic scale. New methods can then be designed to characterize the underlying system of interest at larger and longer scales. An example is to compute the force-extension curve of an actin filament. It was found out that F-actin buckles under compression as an elastic thin rod, and a writhing mode of vibration is developed as a result. Since it only takes a very small force to buckle an actin filament ($\sim$1.68 pN for a 1-μm filament), such a writhing mode of actin could play important roles in the dynamics of F-actin and its interactions with other proteins. These and other features of our CG modeling approach will be explored and reported in the future.

This research was supported by a grant from the National Science Foundation (CHE-0218739) and a Faculty Award from the International Business Machines (IBM) Corporation. The authors also thank the National Science Foundation for TeraGrid resources provided by the National Center for Supercomputing Applications and the National Institutes of Health (grant NCRR 1 S10RR17214-01) on the Arches Metacluster, administered by the University of Utah Center for High Performance Computing.

REFERENCES

1. Howard, J. 2001. Mechanics of Motor Proteins and the Cytoskeleton. Sinauer Associates, Sunderland, MA.
2. Korn, E. D. 1982. Actin polymerization and its regulation by proteins from nonmuscle cells. *Physiol. Rev.* 62:672–737.
3. Sheterline, P., J. Clayton, and J. C. Sparrow. 1998. Actin. Oxford University Press, New York.
4. Tuszynski, J. A., J. A. Brown, and D. Sept. 2003. Models of the collective behavior of proteins in cells: tubulin, actin and motor proteins. *J. Biol. Phys.* 29:401–428.
5. Smith, S. B., L. Finzi, and C. Bustamante. 1992. Direct mechanical measurements of the elasticity of single DNA molecules by using magnetic beads. *Science.* 258:1122–1126.
6. Strick, T. R., J.-F. Allemand, D. Bensimon, A. Bensimon, and V. Croquette. 1996. The elasticity of a single supercoiled DNA molecule. *Science.* 271:1835–1837.
7. Panyukov, S., and Y. Rabin. 2000. Thermal fluctuations of elastic filaments with spontaneous curvature and torsion. *Phys. Rev. Lett.* 85:2404–2407.
8. Panyukov, S., and Y. Rabin. 2000. Fluctuating filaments: statistical mechanics of helices. *Phys. Rev. E.* 62:7135–7146.
9. MacKerell, A. D., D. Bashford, M. Bellott, R. L. Dunbrack, J. D. Evanseck, M. J. Field, S. Fischer, J. Gao, H. Guo, S. Ha, and others. 1998. All-atom emipical potential for molecular modeling and dynamics studies of proteins. *J. Phys. Chem. B.* 102:3586–3616.
10. Brooks, B. R., R. E. Bruccoleri, B. D. Olafson, D. J. States, S. Swaminathan, and M. Karplus. 1983. CHARMM: s program for macromolecular energy, minimization, and dynamics calculations. *J. Comput. Chem.* 4:187–217.
11. Allen, M. P., and D. J. Tildesley. 1987. Computer Simulation of Liquids. Oxford University Press, New York.
12. Graceffa, P., and R. Dominguez. 2003. Crystal structure of monomeric actin in the ATP state: structural basis of nucleotide-dependent actin dynamics. *J. Biol. Chem.* 278:34172–34180.
13. Holmes, K. C., D. Popp, W. Gebhard, and W. Kabsch. 1990. Atomic structure of the actin: DNase I complex. *Nature.* 347:37–44.
14. Otterbein, L. R., P. Graceffa, and R. Dominguez. 2001. The crystal structure of uncomplexed actin in the ADP state. *Science.* 293:708–711.
15. Chu, J. W., and G. A. Voth. 2005. Allostery of actin filaments: molecular dynamics simulations and coarse-grained analysis. *Proc. Natl. Acad. Sci. USA.* 102:13111–13116.
16. Andrianantoandro, E., L. Blanchoin, D. Sept, J. A. McCammon, and T. D. Pollard. 2001. Kinetic mechanism of end-to-end annealing of actin filaments. *J. Mol. Biol.* 312:721–730.
17. Sept, D., J. Y. Xu, T. D. Pollard, and J. A. McCammon. 1999. Annealing accounts for the length of actin filaments formed by spontaneous polymerization. *Biophys. J.* 77:2911–2919.
18. Goetz, R., and R. Lipowsky. 1998. Computer simulations of bilayer membranes: self-assembly and interfacial tension. *J. Chem. Phys.* 108:7397–7409.
19. Marrink, S. J., and A. E. Mark. 2003. Molecular dynamics simulation of the formation, structure, and dynamics of small phospholipid vesicles. *J. Am. Chem. Soc.* 125:15233–15242.
20. Shelley, J. C., and M. Y. Shelley. 2000. Computer simulation of surfactant solutions. *Curr. Opin. Colloid Interface Sci.* 5:101–110.
21. Smit, B., K. Esselink, P. A. Hilbers, N. M. van Os, L. A. M. Rupert, and I. Szleifer. 1993. Computer simulations of surfactant self-assembly. *Langmuir.* 9:9–11.
22. Izvekov, S., and G. A. Voth. 2005. A multiscale coarse-graining method for biomolecular systems. *J. Phys. Chem. B.* 109:2469–2473.
23. Ayton, G., and G. A. Voth. 2002. Bridging microscopic and mesoscopic simulations of lipid bilayers. *Biophys. J.* 83:3357–3370.
24. Ayton, G. S., and G. A. Voth. 2003. Bridged microscopic and mesoscopic computer simulations for biological systems. *Biophys. J.* 84:465A–466A.
25. Wu, Y. H., and J. P. Ma. 2004. Refinement of F-actin model against fiber diffraction data by long-range normal modes. *Biophys. J.* 86:116–124.
26. Ming, D., Y. Kong, Y. Wu, and J. Ma. 2003. Simulation of F-actin filaments of several microns. *Biochem. J.* 85:27–35.

27. Tirion, M. M., D. Benavraham, M. Lorenz, and K. C. Holmes. 1995. Normal-modes as refinement parameters for the F-actin model. *Biophys. J.* 68:5–12.

28. Isambert, H., P. Venier, A. C. Maggs, A. Fattoum, R. Kassab, D. Pantaloni, and M. F. Carliers. 1995. Flexibility of actin filaments derived from thermal fluctuations. *J. Biol. Chem.* 12:11437–11444.

29. Brooks, B. R. 1995. Hatmonic analysis of large systems. I. Methodology. *J. Comput. Chem.* 16:1522–1542.

30. Tirion, M. M. 1996. Large amplitude elastic motions in proteins from a single parameter, atomic analysis. *Phys. Rev. Lett.* 77:1905–1908.

31. Halioglu, T., I. Bahar, and B. Erman. 1997. Gaussian dynamics of folded proteins. *Phys. Rev. Lett.* 79:3090–3093.

32. Bahar, I., and R. L. Jernigan. 1998. Vibrational dynamics of transfer RNAs: comparison of the free and synthetase-bound forms. *J. Mol. Biol.* 281:871–884.

33. Delarue, M., and Y. H. Sanejouand. 2002. Simplified normal mode analysis of conformational transitions in DNA-dependent polymerases: the elastic network model. *J. Mol. Biol.* 320:1011–1024.

34. Zheng, W. J., and S. Doniach. 2003. A comparative study of motor-protein motions by using a simple elastic-network model. *Proc. Natl. Acad. Sci. USA.* 100:13253–13258.

35. Zheng, W. J., and B. Brooks. 2005. Identification of dynamical correlations within the myosin motor domain by the normal mode analysis of an elastic network model. *J. Mol. Biol.* 346:745–759.

36. Ma, J. P. 2005. Usefulness and limitations of normal mode analysis in modeling dynamics of biomolecular complexes. *Structure.* 13:373–380.

37. Hinsen, K., N. Reuter, J. Navaza, D. L. Stokes, and J. J. Lacapere. 2005. Normal mode-based fitting of atomic structure into electron density maps: application to sarcoplasmic reticulum Ca-ATPase. *Biophys. J.* 88:818–827.

38. Tama, F., O. Miyashita, and C. L. Brooks. 2004. Normal mode based flexible fitting of high-resolution structure into low-resolution experimental data from cryo-EM. *J. Struct. Biol.* 147:315–326.

39. Delarue, M., and P. Dumas. 2004. On the use of low-frequency normal modes to enforce collective movements in refining macromolecular structural models. *Proc. Natl. Acad. Sci. USA.* 101:6957–6962.

40. Holmes, K. C., D. Popp, W. Gebhard, and W. Kabsch. 1990. Atomic model of the actin filament. *Nature.* 347:44–49.

41. Orlova, A., and E. H. Egelman. 1992. Structural basis for the destabilization of F-actin by phosphate release following ATP hydrolysis. *J. Mol. Biol.* 227:1043–1053.

42. Orlova, A., and E. H. Egelman. 1993. A conformational change in the actin subunit can change the flexibility of the actin filament. *J. Mol. Biol.* 232:334–341.

43. Orlova, A., A. Shevtsov, V. E. Galkin, D. S. Kudryashov, P. A. Rubenstein, E. H. Egelman, and E. Reisler. 2004. Actin-destabilizing factors disupt filaments by means of a time reversal of polymerization. *Proc. Natl. Acad. Sci. USA.* 101:17664–17668.

44. Egelman, E. H., N. Francis, and D. J. DeRosier. 1982. F-actin is a helix with a random variable twist. *Nature.* 298:131–135.

45. Humphrey, W., A. Dalke, and K. Scholten. 1996. VMD: visual molecular dynamics. *J. Mol. Graph.* 14:33–38.

46. Yasuda, R., H. Miyata, and K. J. Kinosita. 1996. Direct measurement of the torsional rigidity of single actin filaments. *J. Mol. Biol.* 263:227–236.

47. Ben-Avraham, D., and M. M. Tirion. 1995. Dynamic and elastic properties of F-actin: a normal-modes analysis. *Biophys. J.* 68:1231–1245.

48. Durand, P., G. Trinquier, and Y. H. Sanejouand. 1994. New approach for determining low-frequency normal-modes in macromolecules. *Biopolymers.* 34:759–771.

49. Go, N. 1990. A theorem on amplitudes of thermal atomic fluctuations in large molecules assuming specific conformations calculated by normal mode analysis. *Biophys. Chem.* 35:105–112.

50. Bustamante, C., Y. R. Chemla, N. R. Forde, and D. Izhaky. 2004. Mechanical processes in biochemistry. *Annu. Rev. Biochem.* 73: 705–748.

51. Mehta, A. D., M. Rief, J. A. Spudich, D. A. Smith, and R. M. Simmons. 1999. Single-molecule biomechanics with optical methods. *Science.* 283:1689–1695.

52. Wang, M. D. 1999. Manipulation of single molecules in biology. *Curr. Opin. Biotechnol.* 10:81–86.

53. Kojima, H., A. Ishijima, and T. Yanagida. 1994. Direct measurement of stiffness of single actin filaments with and without tropomyosin by in vitro nanomanipulation. *Proc. Natl. Acad. Sci. USA.* 91:12962–12966.